Effect of lithium–sodium mixed-alkali on phase transformation kinetics in Er^{3+}/Yb^{3+} co-doped aluminophosphate glasses

Yongzheng Fang [a,b,c,*], Meisong Liao [a], Lili Hu [a]

[a] *Shanghai Institute of Optics and Fine Mechanics, Chinese Academy of Sciences, 390 Qinghe Road, Jiading District, Shanghai 201800, China*
[b] *Graduate School of the Chinese Academy of Sciences, Beijing 100039, China*
[c] *Shanghai Institute of Technology, Shanghai 200235, China*

Abstract

Er^{3+} doped aluminophosphate glasses with various Na_2O/Li_2O ratios were prepared at $1250\,°C$ using a silica crucible to study mixed alkali effect (MAE). The effect of relative alkali content on glass transition temperature, crystallization temperature and thermal stability were investigated using differential scanning calorimetry (DSC). In addition, apparent activation energies for crystallization, E_c, were determined employing the Kissinger equation. The effect of Al_2O_3 content on the magnitude of MAE was also discussed. No mixed-alkali effect is observed on crystallization temperature.
© 2006 Elsevier B.V. All rights reserved.

Keywords: Mixed alkali effect; DSC; Crystallization; Kinetics

1. Introduction

Mixed alkali glasses contain more than one type of modifying cation. A number of mixed alkali glass systems demonstrate non-linearity in electrical conductivity, viscosity, thermal properties, and chemical durability [1–3]. This non-linear behavior in glass systems as a function of composition is very different from the behavior of single modifier oxide glass systems, where approximate linear trends are observed. Many physical properties measured in mixed-alkali systems show initial non-linear growth and subsequent reversal in trends leading to maxima or minima as a function of modifier fraction. This phenomenon is known as the 'mixed alkali effect', and there exist both technological and theoretical interests in describing the physics and chemistry of mixed-alkali glasses. This pronounced effect has attracted the attention of many scientists with most of their work compiled in [4–6]. Besides older explanations of the mixed alkali effect [7,8], there have been a variety of recent ones [9–11]. These models assumed either large structural modifications induced by mixing mobile species of different sizes or specific interaction between these dissimilar mobile species. Nevertheless, these proposed models are not satisfactory so far, even if they are physically sound they contain too many unknown parameters to allow a reliable quantitative evaluation of the huge amount of measured data [12]. Furthermore, most of these empirical equations are only valid for glasses within certain range of composition and viscosity values. The mixed alkali phenomenon, which from a practical viewpoint is useful in manufacturing low-loss electrical glass and in understanding chemical strengthening of glass, is not completely understood, thereby necessitating further in-depth characterizations of mixed alkali materials.

The purpose of the present paper is to investigate the effect of mixed alkali additions on the thermal transformation and crystallization kinetics of Er^{3+}/Yb^{3+} co-doped aluminophosphate glasses. Erbium laser glasses have attracted much attention due to their capability for emission at the eye-safe wavelengths and optical communication windows of $1.54\,\mu m$ [13]. Phosphate glasses have attracted considerable interest in recent years because of their technological interest, especially in optical [14] and biomaterial applications [15]. Moreover, phosphate glass is considered to be the best matrix for ytterbium sensitized erbium glass laser because of its high stimulated emission cross-section, weak up-conversion luminescence and low probability of energy backtransfer from Er^{3+} to Yb^{3+}. The ability to control the

---

* Corresponding author. Tel.: +86 21 59911204; fax: +86 21 39910393.
E-mail address: fangyzh@yahoo.com.cn (Y. Fang).

crystallization of different vitreous matrices permits the glass synthesis under ideal conditions. Consequently, it is important to know the physical and thermal characteristics of interest. The understanding of the micromechanism of crystallization is a prerequisite for most of the applications, as stability against crystallization determines their effective working limits.

2. Experimental

In the present work, Er^{3+} doped phosphate glasses of the type $xNa_2O–(15 − x)Li_2O–4B_2O_3–11Al_2O_3–5BaO–65P_2O_5$ (where $x = 0$, 3.75, 7.5, 11.25 and 15 mol%) were used to investigate the effect of mixed alkali on thermal transformation and crystallization kinetics of glasses. To this glass were externally added Er_2O_3 and Yb_2O_3 at 0.5 and 2 mol% level, respectively. Er^{3+} was active ion for 1.54 μm laser in glass substrates and Yb^{3+} was introduced as sensitizer. All chemicals were reagent grade and obtained from different standard companies with 99.99% purity. The raw materials in 500 g batches were thoroughly mixed and ground in an agate mortar. The mixtures were then melted in a silica crucible at 1200 °C and kept at their melting temperatures for about 1 h with occasional stirring to ensure homogeneity. Then, the melts were quickly quenched between two well-polished steel plates.

Differential scanning calorimetry (DSC) Setram TG-DSC 1600 was used to measure the caloric manifestation of the crystallization and to study the crystallization kinetics. The temperature precision of this equipment was ±0.1 K with an average standard error of about ±1 K in the measured values. The DSC runs were taken at six different heating rates, i.e. 1, 5, 10, 15, 20 and 25 K/min on $30 ± 1$ mg powder samples sized <210 μm under a flowing (50 cm^3 min^{-1}) atmosphere of dry air. The DSC equipment was calibrated prior to measurements, using high purity standards Pb, Sn, In and Al with well-known melting points. Pure Al_2O_3 was used as a standard.

Apparent activation energy for crystallization, E_c, was determined from the variation in peak crystallization temperature with heating rate employing the Kissinger equation [16]:

$$\ln(T_p^2/a) = E_c/RT_p + \text{constant}$$

where T_p is the temperature of the maximum DSC crystallization peak, a the heating rate, and R is the universal gas constant. The activation energy E_c was calculated from the slopes of the linear fit to the experimental data from a plot of $\ln(T_p^2/a)$ versus $1/T_p$.

3. Results and discussions

A typical DSC thermogram of glasses at a heating rate of 10 K/min is shown in Fig. 1 for different x-values, the proportion of Na_2O. As the DSC diagrams at other heating rates are similar in shape, they have not been shown. From the analysis point of view, the DSC thermogram is divided into two parts. The first one corresponds to the glass transition region represented by endothermic reaction and the other part is related to the crystallization process indicated by exothermic part of DSC curve. From Fig. 1 we can easily see the three characteristic temperatures, the extrapolated on-set glass transition (T_g),
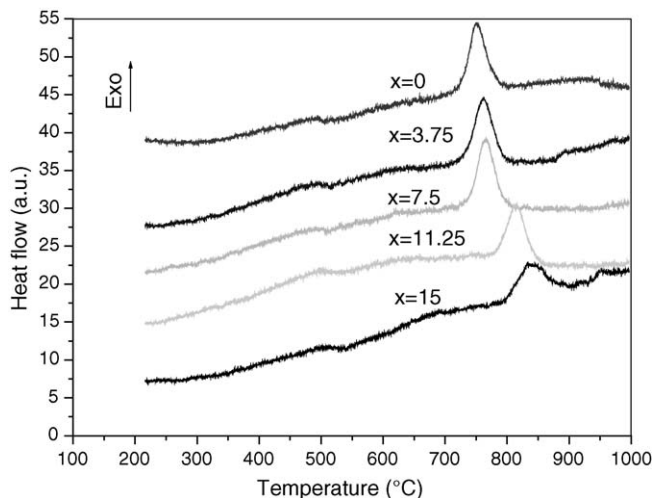

Fig. 1. Typical DSC curves of $xNa_2O–(15 − x)Li_2O–4B_2O_3–11Al_2O_3–5BaO–65P_2O_5$ ($x = 0$, 3.75,7.5,11.25 and 15 mol%) glasses heated at a constant rate 10 K/min.

the extrapolated on-set temperature of crystallization (T_0), and the peak temperature for crystallization (T_p). A measure of the thermal stability of each glass was made from the temperature difference, ΔT_{TS}, between T_g and T_0. The greater this temperature difference, the greater is the thermal stability of the system.

The variations of T_g, T_0 and ΔT_{TS} with the relative alkali ratio $Na/(Na + Li)$ are shown in Figs. 2 and 3. T_g plotted as a function of the relative alkali ratio exhibits a non-linear behavior and reached a minimum at $Na/(Na + Li) = 0.5$, as usually observed [17]. In literature, T_g does not exhibit systematically a MAE [18], nevertheless, it was already shown that the MAE could considerably affect this property in different systems like in Na/Li tellurite [19], Na/Li metaphosphate [20], Ag/Rb chalcogenide glasses [21] and Na/K aluminoborosilicate glasses [22]. There the mobility of the larger ion is reduced because the presence of the smaller ion leads to an increasing packing density of oxygen atoms, i.e. the mesh size of the silicate network is reduced when
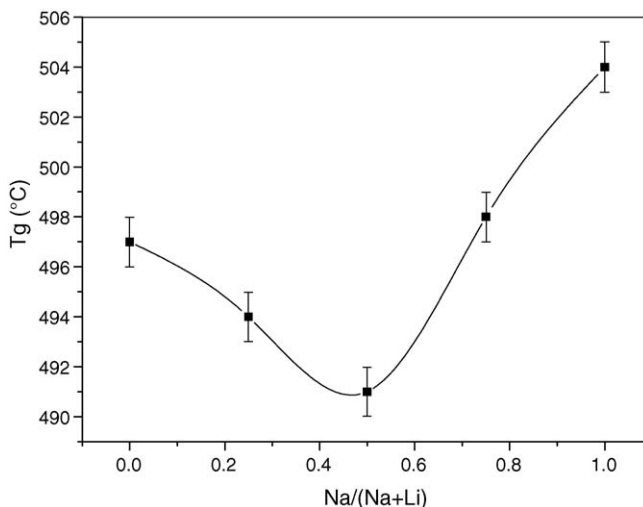

Fig. 2. Variation of glass transition T_g as function of the relative alkali ratio of $Na/(Na + Li)$.
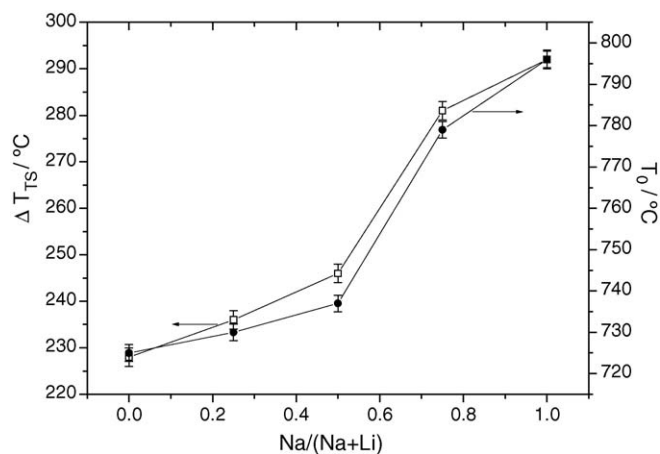
Fig. 3. Variations of on-set crystallization temperature T_0 and glass thermal stability parameter ΔT_{TS} as function of the relative alkali ratio of Na/(Na + Li).

Fig. 4. The plot of $\ln(T_p^2/a)$ against $1000/T_p$ for evaluation of the crystallization activation energy, E_c, for xNa$_2$O–$(15 - x)$Li$_2$O–4B$_2$O$_3$–11Al$_2$O$_3$–5BaO–65P$_2$O$_5$ ($x = 0$, 3.75, 7.5, 11.25 and 15 at.%) glasses.

compared with the one containing the larger cations only. Compared to the network which contains the smaller ions only, the small ions experience an expanded mesh size in the mixed glass and, therefore, their mobility should be increased in the mixed case that is in the mechanisms responsible for the MAE. The minimum of T_g can also be interpreted in terms of an increase of non-bridging oxygen (NBO) in the glass structure.

A more interesting observation is that the T_g is higher and the magnitude of the mixed alkali effect (corresponding to the departure from additivity in T_g) is much smaller comparing with the 0.46 [xNa$_2$O$(1 - x)$Li$_2$O, 0.54P$_2$O$_5$] glass studied in Ref. [17]. This phenomenon can be explained by the higher Al$_2$O$_3$ content in the glasses investigated in the present work. Adding Al$_2$O$_3$ results in an increase of T_g as already observed in phosphate glasses [23]. But again we can observe a decrease in the magnitude of the MAE when Al$_2$O$_3$ content increases. This shows that the presence of Al$_2$O$_3$ appears to act on the mechanisms responsible for the MAE. Al$_2$O$_3$ increases the covalency of P–O bonds and that there is a strengthening of the glass structure through the formation of aluminophosphate bonds. This network strengthening is consistent with the glass transition moving toward higher temperature as alumina content increases. NMR spectra [24] reveal that octahedrally coordinated Al(OP)$_6$ is the predominant configuration of Al in similar glasses. The formation of Al(OP)$_6$ polyhedra in aluminophosphate glasses obviously modifies the cation environment and the number of non-bridging oxygens should decrease [25]. The types of oxygen to which alkali ions are coordinated are consequently modified in aluminophosphate glasses. These modifications are also crucial in specifying the cation environment. The type of cation environment, and especially the non-bridging oxygens may play an important role in the limitation of the ionic migration in mixed alkali glasses. In addition, the strengthening of the network could limit the adaptability of the cation environment, which is the key aspect of the two recent models dynamic structure model (DMS) [26] and random distribution model (RDM) [27] to explain the MAE, and inhibit the mechanisms responsible for it. The main idea of the DSM model is the existence of mismatches between the different types of sites designed by cations in the glass. Ionic
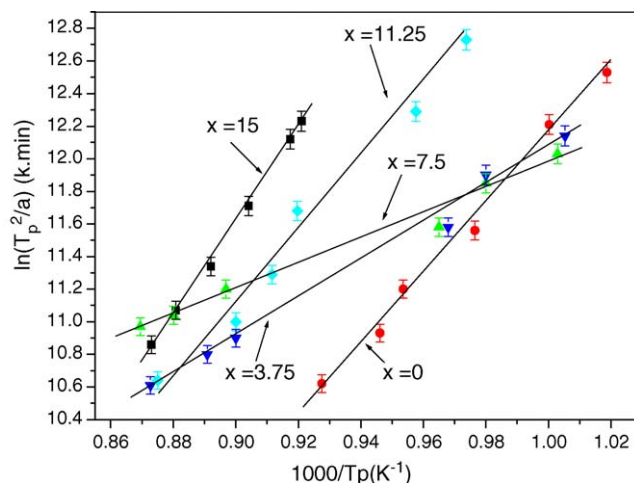
migration is associated with a "memory effect" of the sites previously occupied, which leads to the creation of ionic pathways. The random distribution model (RDM) is based on almost the same arguments.

However, mixing two alkali oxides does not affect T_0 and ΔT_{TS}, as observed in Fig. 3. T_0 and ΔT_{TS} do not show minimum as function of relative alkali ratio. It shows that there is no effect of mixed alkali additions on glass properties at high temperature [28,29].

Fig. 4 shows plots of $\ln(T_p^2/a)$ versus $1000/T_p$ for glass samples with different relative alkali ratio. As described before, the activation energy E_c was calculated from linear fits to the experimental data using the Kissinger equation. Calculated values for different glasses were also showed in Fig. 5 as a function of relative alkali ratio. The active energy minimum of crystallization is about 60.7 kJ/mol when the relative alkali ratio Na/(Na + Li) is 0.5.

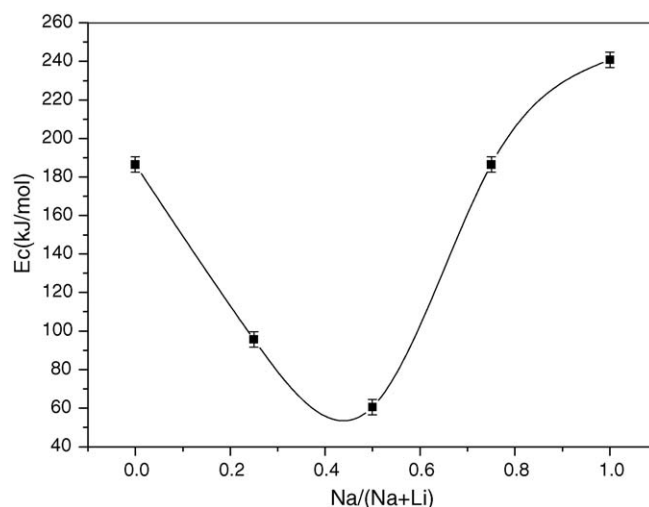Fig. 5. Variations of crystallization activation energy, E_c, as function of the relative alkali ratio of Na/(Na + Li).

4. Conclusions

In this paper, we measured the caloric manifestation of glass transition and the crystallization of erbium doped mixed lithium–sodium aluminophosphate glasses with different relative alkali ratio using differential scanning calorimetry. In addition, the kinetics of crystallization of glasses was also investigated. As demonstrated by T_g measurements, glasses exhibited a mixed alkali effect (MAE). Due to high content of Al_2O_3 in all glasses, glasses showed high T_g and small magnitude of the mixed alkali effect. There was no mixed alkali effect on properties at high temperature, as showed by on-set temperature of crystallization.

Acknowledgements

References

[1] D.E. Day, J. Non-Cryst. Solids 21 (1976) 343.
[2] A.H. Dietzel, Phys. Chem. Glasses 24 (1983) 172.
[3] M. Ingram, Glastech. Ber. 67 (1994) 151.
[4] K. Hughes, J.O. Isard, in: J. Hladik (Ed.), Physics of Electrolytes, vol. 1, Academic Press, London, 1972, p. 387.
[5] G.H. Frischat, Ionic Diffusion in Oxide Glasses, TransTech, Aedermansdorf, 1975, p. 161.
[6] M.D. Ingram, in: R.W. Cahn, P. Haasen, E.J. Kramer (Eds.), Materials Science and Technology, vol. 9, VCH, New York, 1991, p. 715.
[7] R.L. Myuller, Zr. Tek. Fiz. 25 (1955) 236.
[8] J.R. Hendrickson, P.J. Bray, Phys. Chem. Glasses 13 (1972) 43.
[9] K. Funke, Prog. Solid State Chem. 22 (1993) 111.
[10] P. Maass, A. Bunde, M.D. Ingram, Phys. Rev. Lett. 68 (1992) 3064.
[11] J.E. Davidson, M.D. Ingram, A. Bunde, K. Funke, J. Non-Cryst. Solids 203 (1996) 246.
[12] R. Kirchheim, J. Non-Cryst. Solids 328 (2003) 157.
[13] V. Fromzel, et al., Solid state lasers and new laser materials, SPIE 1839 (1991) 166.
[14] M.J. Weber, J. Non-Cryst. Solids 123 (1990) 208.
[15] B. Kumar, S. Li, J. Am. Ceram. Soc. 74 (1991) 226.
[16] H.E. Kissinger, J. Res. Natl. Bur. Stand. 57 (1956) 217.
[17] A. Faivre, D. Viviani, J. Phalippou, Solid State Ionics 176 (2005) 325.
[18] F.C.A.V. Ali, G.N. Greaves, M.C. Jermy, K.L. Ngai, M.E. Smith, Solid State Nucl. Magn. Reson. 5 (1995) 133.
[19] P. Balaya, C.S. Sunandana, J. Non-Cryst. Solids 175 (1994) 51.
[20] R.K. Sato, R.J. Kirkpatrcik, R.K. Brow, J. Non-Cryst. Solids 143 (1992) 257.
[21] C.A.P. Rau, A. Pradel, C.P.E. Varsamis, E.I. Kamitsos, D. Granier, A. Ibanez, E. Philippot, Phys. Rev. B 63 (2001) 184204.
[22] N. Ollier, T. Charrpentier, B. Boizot, G. Wallez, D. Ghaleb, J. Non-Cryst. Solids 341 (2004) 26.
[23] R.K. Brow, J. Am. Ceram. Soc. 76 (1993) 913.
[24] R.K. Brow, R.J. Kirkpatrick, L.T. Turner, J. Am. Ceram. Soc. 76 (1993) 919.
[25] R.K. Brow, R.J. Kirkpatrick, L.T. Turner, J. Am. Ceram. Soc. 73 (1990) 2293.
[26] P. Maass, A. Bunde, M.D. Ingram, Phys. Rev. Lett. 68 (1992) 3064.
[27] J. Swenson, et al., Phys. Rev. B 63 (2001) 132202.
[28] C.T. Moynihan, N.S. Saad, D.C. Tran, A.V. Lesikar, J. Am. Ceram. Soc. 63 (1980) 458.
[29] M. Tomozawa, V. McGahay, J. Non-Cryst. Solids 128 (1991) 48.